Title

Involvement of AtNAP1 in the regulation of chlorophyll degradation in *Arabidopsis thaliana*

Tomohiro Nagane, Ayumi Tanaka, Ryouichi Tanaka

Institute of Low Temperature Science, Hokkaido University, N19W8, Kita-ku, Sapporo 060-0819, Japan

Corresponding author

Ryouichi Tanaka

e-mail: rtanaka@lowtem.hokudai.ac.jp; Tel: +81 11 706 5496, Fax: +81 11 706 5493

Abstract

In plants, chlorophyll is actively synthesized from glutamate in the developmental phase and degraded into non-fluorescent chlorophyll catabolites during senescence. The chlorophyll metabolism must be strictly regulated because chlorophylls and their intermediate molecules generate reactive oxygen species. Many mechanisms have been proposed for the regulation of chlorophyll synthesis including gene expression, protein stability and feedback inhibition. However, information on the regulation of chlorophyll degradation is limited. The conversion of chlorophyll *b* to chlorophyll *a* is the first step of chlorophyll degradation. In order to understand the regulatory mechanism of this reaction, we isolated a mutant which accumulates 7-hydroxymethyl chlorophyll *a* (HMChl), an intermediate molecule of chlorophyll *b* to chlorophyll *a* conversion, and designated the mutant *hmc1*. In addition to HMChl, *hmc1* accumulated pheophorbide *a*, a chlorophyll degradation product, when chlorophyll degradation was induced by dark incubation. These results indicate that the activities of HMChl reductase (HAR) and pheophorbide *a* oxygenase (PaO) are simultaneously down-regulated in this mutant. We identified a mutation in the *AtNAP1* gene, which encodes a subunit of the complex for iron-sulfur cluster formation. HAR and PaO use ferredoxin as a reducing power and PaO has an iron-sulfur center; however, there were no distinct differences in the protein levels of ferredoxin and PaO between wild type and *hmc1*. The concerted regulation of chlorophyll degradation is discussed in relation to the function of AtNAP1.

Keywords: *Arabidopsis thaliana*, chlorophyll metabolism, plastid

Abbreviations

CAO Chlorophyllide *a* oxygenase

HMChl 7-Hydroxymethyl chlorophyll *a*

HAR 7-Hydroxymethyl chlorophyll *a* reductase

LHCII Light-harvesting chlorophyll *a*/*b*-protein complexes of photosystem II

PaO Pheophorbide *a* oxygenase

ROS Reactive oxygen species

Introduction

Chlorophyll molecules participate in the initial and indispensable processes of photosynthesis such as harvesting light energy and driving electron transfer (Green and Durnford 1996; Fromme et al. 2003). Chlorophyll is actively synthesized during the greening phase for the formation of photosystems (Shimada et al. 1990) and, in contrast, chlorophyll is converted to safety molecules during senescence (Hörtensteiner 2006). In green leaves, synthesis and degradation of chlorophyll are necessary for the maintenance of photosystems because photosynthesis machineries turn over in green leaves. Among various photosynthetic components, core chlorophyll-protein complexes of photosystem II (D1) rapidly turn over during photosynthesis (Vasilikiotis and Melis 1994). Chlorophyll metabolic activity is also observed during acclimation to changes in light intensity in order to control the amount of absorbed light energy (Masuda et al. 2002; Harper et al. 2004; Pattanayak et al. 2005).

In higher plants, chlorophyll is synthesized from glutamate (Tanaka and Tanaka 2007) and degraded into safety molecules of non-fluorescence chlorophyll catabolites (Hörtensteiner 2006). Chlorophyll must be synthesized according to the demand of photosystems. In addition, free chlorophyll and its intermediate molecules produce reactive oxygen species (ROS) under illumination (op den Camp et al. 2003). If there is excessive accumulation of chlorophyll

intermediate molecules, a large amount of ROS might be possibly generated, resulting in growth retardation and cell death. Chlorophyll intermediate molecules are also postulated to be an important signal for cellular processes such as the cell cycle (Kobayashi et al. 2009). For these reasons, chlorophyll metabolism is strictly regulated by various mechanisms such as gene expression (Matsumoto et al. 2004), feedback inhibition (Vothknecht et al. 1998) and protein stability (Yamasato et al. 2005).

At the last step of chlorophyll synthesis, chlorophyll *a* is converted to chlorophyll *b* (Tanaka et al. 1998) and chlorophyll *b* is reconverted to chlorophyll *a* (Ito et al. 1993). This interconversion pathway is called the chlorophyll cycle (Rüdiger 2002). This cycle has some important physiological roles. When plants are transferred from low light to high light conditions, light-harvesting chlorophyll *a*/*b*-protein complexes of photosystem II (LHCII) are degraded and the chlorophyll *a/b* ratio increases in order to reduce antenna sizes (Yang et al. 2001; Tanaka and Tanaka 2005). In this process, the chlorophyll *b*-to-chlorophyll *a* conversion most likely takes place to balance the chlorophyll *a/b* ratios (Masuda et al. 2003; Tanaka and Tanaka 2005). In contrast, chlorophyll *b* synthesis is accelerated (Harper et al. 2004) when plants acclimate to low light intensities in order to increase LHCII levels. As mentioned above, the chlorophyll *b*-to-chlorophyll *a* conversion is the initial step of chlorophyll *b* degradation (Hörtensteiner 2006; Kusaba et al. 2007).

Chlorophyll *b* is synthesized from chlorophyll *a* by chlorophyllide *a* oxygenase (CAO) (Tanaka et al. 1998). CAO belongs to the Rieske non-heme iron oxygenase family and it carries out two successive oxygenation reactions and converts chlorophyll *a* to chlorophyll *b* via HMChl (Oster et al. 2000). The regulation of this enzyme has been extensively studied. CAO has an N-terminal extension called the A domain which regulates the accumulation of CAO protein in response to accumulation of chlorophyll *b* (Yamasato et al. 2005; Nakagawara et al. 2007; Sakuraba et al. 2007). CAO is also regulated at a transcriptional level and the expression of CAO gene is modulated by light

intensities (Masuda et al. 2003; Tanaka and Tanaka 2005). By these transcriptional and post-translational regulation mechanisms, chlorophyll *b* synthesis is finely controlled. Chlorophyll *b* is reconverted to chlorophyll *a* via HMChl (Ito et al. 1996). This reaction is not the reverse reaction of CAO but is catalyzed by at least two different enzymes. The first enzyme, chlorophyll *b* reductase, was recently identified with a rice stay-green mutant (Kusaba et al. 2007). Chlorophyll *b* and LHCII are selectively stabilized in this mutant. In vitro experiments showed that chlorophyll *b* reductase converts not only free chlorophyll *b* but also chlorophyll *b* in LHCII to HMChl (Horie et al. 2009), suggesting that chlorophyll *b* reductase participates in the initial step of LHCII degradation. On the other hand, the second enzyme for chlorophyll *b* to chlorophyll *a* conversion, HAR, has not been identified yet. The enzyme requires reduced ferredoxin and the activity was shown to be associated with thylakoid membranes (Ito et al. 1994; Scheumann et al. 1998). However, information of this enzyme is limited because our knowledge of this enzyme is based only on result obtained from experiments with plastids or its membranes.

Recently, molecular genetics has become one of the most powerful tools for study of chlorophyll metabolism. A large number of enzymes responsible for chlorophyll metabolism have been identified (Ito et al. 1994; Scheumann et al. 1998) and novel regulatory mechanisms have been elucidated by using mutants. In this study, we isolated a mutant which accumulates HMChl, an intermediate molecule between chlorophyll *a* and chlorophyll *b*. Interestingly, this mutant accumulated pheophorbide *a*, a chlorophyll degradation product, when chlorophyll degradation was induced by dark incubation. By a genetic approach, we found that the conversion of HMChl to chlorophyll *a* is partly impaired in this mutant. We identified a mutation in the *AtNAP1* gene, which has been proposed to encode a subunit of a system for iron-sulfur cluster formation (Xu et al. 2005). The concerted regulation of chlorophyll degradation is discussed.

Materials and methods

Plant material and growth conditions

The wild-type *Arabidopsis thaliana* (Columbia ecotype) and all of the *Arabidopsis* mutants described in the Results section were grown for 3 weeks in a chamber equipped with white fluorescent lamps (FLR40SSW, NEC Co. Ltd., Tokyo, Japan) under continuous illumination at a light intensity of 100 uE m^{-2} s^{-1} at 22°C on a 1:1 mixture of vermiculite and nourished soil (Sankyo-Baido soil, Hokkai-Sankyo Co. Ltd., Kita-Hiroshima, Japan). The plants were subsequently transferred to darkness for 5 d at 22°C for chlorophyll degradation experiments. The third leaf whorl was harvested at the time indicated in the Results section and immediately frozen in liquid nitrogen for pigment analysis. For electron microscopy, the fourth leaf whorl counting down from the top of the plant was harvested and immediately soaked in primary fixation solution (1% paraformaldehyde, 2.5% glutaraldehyde in 50 mM PIPES buffer, pH 7.2, containing 0.1 M sucrose).

The *pao1* (SALK_111333) and *nyc1* (SALK_091664) mutants were obtained from the Arabidopsis Biological Resource Center (http://www.biosci.ohio-state.edu/pcmb/Facilities/abrc/abrchome.htm), and the *nol* (AL759262) mutant was obtained from GABI-KAT (Cologne, Germany).

Positional cloning of *HMC1*

The homozygous *hmc1* mutant obtained by ethyl methanesulfonate treatment was crossed to the Lansberg *erecta* wild-ecotype. Genomic DNA from homozygous *hmc1* F2 plants was extracted and used for initial mapping utilizing simple sequence length polymorphism and cleaved amplified polymorphic sequence markers distributed over the five

chromosomes (http://www.arabidopsis.org/). To narrow down the region of the *HMC1* locus, new markers were designed on the basis of insertion/deletion information obtained from the Monsanto Web site (https://www.ncgr.org/cgi-bin/cereon/cereon_login.pl).

Complementation of the *hmc1* mutant

For complementation of the *hmc1* mutation, PCR fragments containing the *AtNAP1* (At4g04770) gene were amplified using genomic DNA extracted from wild-type Columbia. The amplified gene region was then sub-cloned into the pGreenII-0029 plasmid (Hellens et al. 2000). We incorporated the 35S promoter of the Cauliflower mosaic virus and the Tobacco mosaic virus omega sequence (Prof. Y. Niwa, University of Shizuoka) into this vector for efficient overexpression of the transgene. Homozygous *hmc1* plants were transformed with the *Agrobacterium tumefaciens* strain GV2260 and transformants were selected on plates containing half-strength MS medium, 0.7% agarose, and 50 mg mL^{-1} kanamycin. The successfully grown transgenic plants were then transferred to soil pots and were subsequently grown with a 16-h photoperiod at 23°C.

Electron microscopy

Arabidopsis leaves were harvested under dim green light and immediately soaked in the primary fixation buffer described above. Samples were rinsed in 50 mM PIPES buffer (pH 7.2, three 15-min rinses) and subsequently dehydrated in a graded series of ethanol dilutions (30, 50, 70, 90, 100% x 3, v/v) for 15 min at each dilution. Samples were embedded in an Epon resin mixture (TAAB Epon 812, TAAB Laboratories Equipment Ltd, Berkshire, U.K.). Ultra-thin sections were mounted on 100-mesh size grids. Specimens were stained for 20 min with 2% (w/v) aqueous

uranyl acetate and briefly with lead citrate, washed under a gentle stream of water, and viewed with a JOEL 1200EX transmission electron microscope (JOEL Ltd., Tokyo, Japan) operating at 100 kV.

Pigment analysis

Leaves were weighed and pulverized in acetone using a ShakeMaster grinding apparatus (BioMedical Science Co. Ltd., Tokyo, Japan). Extracts were centrifuged for 10 min at 10,000 x g and the supernatant was mixed with water for a final acetone concentration of 80%. Pigments were separated on a Symmetry C8 column (150 mm in length, 4.6 mm in i.d.; Waters, Milford, MA) according to the method of Zapata et al. (Zapata et al. 2000). Elution profiles were monitored by measuring absorbance at 659 nm. Standard pigments (chlorophyll *a* and chlorophyll *b*) were purchased from Juntec Co. Ltd. (Odawara, Japan). HMChl was prepared as described previously (Ito et al. 1996).

Immunoblot analysis

Total protein was extracted from leaves by grinding with extraction buffer (50 mM Tris (pH 6.8), 10% glycerol, 2% SDS, and 6% 2-mercaptoethanol). After grinding, the homogenates were centrifuged at 10,000 x g for 5 min and the supernatants were separated with SDS-PAGE and subsequently electro-transferred onto a Hybond-P membrane (GE Healthcare UK Ltd., Buckinghamshire, England). Proteins were labeled with an anti-ferredoxin antibody (AgriSera, Vännäs, Sweden) or with anti-PaO or -AtNAP1 antibody prepared in our laboratory against recombinant PaO and AtNAP1 proteins, respectively. Antibodies were detected using the ECL plus Western blotting detection system (GE Healthcare) according to the manufacturer's instructions.

Results

Isolation of a mutant accumulating HMChl

Figure 1 shows an overview of the chlorophyll cycle. Among the enzymes involved in the chlorophyll cycle HAR is not yet identified. HMChl is an intermediate molecule between chlorophyll *a* and chlorophyll *b*. If HAR is inactivated, the precursor of this enzyme, HMChl, should accumulate. In order to isolate mutants in which HAR activity is compromised, we germinated ethyl methanesulfonate-mutagenized seeds and examined their pigment compositions by HPLC. The wild type and the majority of the lines accumulated only chlorophyll *a* and chlorophyll *b*, and their intermediate molecules were not detected or were at very low levels. Among 7,000 lines examined, two lines exhibited an additional peak of a chlorophyll derivative on the HPLC profile (Fig. 2a). Absorbance maxima in red and blue regions of this pigment were 434 nm and 659 nm, respectively (Online Resource 1a) and the retention time of this pigment was 31 min. These characteristics were identical to those of the authentic HMChl standard, indicating that these lines accumulate HMChl. One of the two mutants in which the HMChl level was higher was designated as *hmc1* for 7-hydroxymethyl-chlorophyll accumulation and used for further analysis. Another mutant accumulated only a small amount of HMChl (data not shown), thus, this mutant was not subjected to further analysis. The *hmc1* mutant was recessive. It accumulated no or barely detectable amounts of other intermediate molecules of chlorophyll biosynthesis such as Mg-proto IX and Proto IX in the green leaves. Accumulation of intermediate molecules of chlorophyll metabolism is usually accompanied by necrosis or cell death. Although *hmc1* accumulated a significant amount of HMChl corresponding to about 1-2% of total chlorophyll, the mutant exhibited no necrotic or bleaching phenotypes (Fig. 2b). The size of the cotyledons and leaf numbers were almost the same as those of the wild type, but *hmc1* exhibited a slow growth rate and the small leaf size compared to those of the wild type. HMChl gradually increased as

the developmental stage proceeded and then decreased during senescence in *hmc1*. The HMChl level was very low throughout the period of development in the wild type (Fig. 3a). Chlorophyll contents per g fresh weight increased and reached the maximum level at 20 days after germination and then decreased during senescence in the wild type (Fig. 3b). In the *hmc1* mutant, chlorophyll contents slowly increased and the maximum level was slightly lower than that of the wild type. The wild type and *hmc1* mutant exhibited the same trends in chlorophyll *a/b* ratios during development (Fig. 3c).

Reduction in the HMChl-to-chlorophyll *a* activity in *hmc1*

HMChl is an intermediate molecule of both the chlorophyll *a*-to-chlorophyll *b* conversion and the chlorophyll *b*-to-chlorophyll *a* conversion. To determine which reaction in the chlorophyll cycle causes HMChl accumulation in the *hmc1* mutant, we crossed this mutant with the *nyc1/nol* double mutant (Horie et al. 2009), which completely lacks chlorophyll *b* reductase. If reduction in HAR activity is the cause of HMChl accumulation, the absence of chlorophyll *b* reductase should result in suppression of HMChl accumulation in the *hmc1/nyc1/nol* triple mutant. In contrast, if impairment in CAO activity is responsible for HMChl accumulation, the triple *hmc1/nyc1/nol* mutant should accumulate a level of HMChl equivalent to that in the *hmc1* mutant. In the triple mutant, we found that the accumulation of HMChl was suppressed to the wild type level (Fig. 4). These results indicated that HMChl accumulated due to impairment in HAR activity. Interestingly, the triple mutant showed growth retardation and low pigmentation like the *hmc1* mutant, indicating that these phenotypes were not the result of HMChl accumulation.

Accumulation of pheophorbide *a* in *hmc1* during dark incubation

In order to examine whether the mutation affects not only the chlorophyll cycle but also other reactions, green plants were transferred to darkness and the chlorophyll degradation process was examined. No degradation product was found in wild-type leaves after 5 days of dark incubation; in contrast, pheophorbide *a*, an intermediate of chlorophyll degradation (Fig. 1; see Online Resource 1b for its absorption spectrum), and HMChl accumulated in the *hmc1* mutant (Fig. 5). The level of HMChl in *hmc1* during senescence (Fig. 5) was slightly lower than that under the normal condition (Fig. 4). This finding appears puzzling, as one would expect an increase in the HMChl levels during senescence rather than a decrease, if HAR activity decreased in the *hmc1* mutant. An explanation for this observation will be a possible increase in the level of HAR during senescence. Though the activity of HAR is likely to be reduced by the *hmc1* mutation, plants may be able to compensate the loss of the activity by increasing the HAR protein level. Another explanation will be possible inhibition of the activity of chlorophyll *b* reductase by impairment of PaO activity. Such a feedback mechanism is proposed based on the studies on *pao* mutants (Hörtensteiner, 2009).

The amount of accumulated pheophorbide *a* in *hmc1* corresponded to more than 40% of degraded chlorophylls and to about 22% of the total chlorophylls that accumulated before dark treatment in this mutant (Online resource 2). These findings indicate that the *hmc1* mutation affects specific steps in both the chlorophyll cycle and the degradation pathway. We also found an interesting visible phenotype of *hmc1* after dark incubation. After 5 days of dark incubation, wild-type plants were still intact, although old leaves had become yellow. In contrast, *hmc1* leaves had become crinkled and retained green (data not shown). The *hmc1* mutant showed a cell-death phenotype after dark treatment, which phenotype resembled to that of the *pao* mutant. The other phenotypes were not shared by these two mutants. The *pao* mutant was not pale green unlike *hmc1*, and the leaves of the *pao* mutant occasionally turn whitish even under

normal growth conditions (data not shown), which was not the case with the *hmc1* mutant. Next, we examined the cell structure by electron microscopy (Fig. 6). Significant differences were not observed between wild type and *hmc1* before dark incubation. When wild-type plants were incubated in the dark for 5 days, chloroplasts became round, but the integrity of membrane systems such as the chloroplast envelope, thylakoid membranes, tonoplast and plasma membranes were not changed. However, when the *hmc1* plants were incubated in the dark, all of these cellular membrane structures were disrupted. These phenotypes were similar to the *pao* mutant in which PaO activity was compromised and pheophorbide *a* was accumulated upon senescence (Hirashima et al. 2009). Therefore, we speculate that the phenotype of *hmc1* in darkness was mainly due to the accumulation of pheophorbide *a*.

Map-based cloning of the *hmc1* locus

For genetic mapping of the *hmc1* locus, we crossed the *hmc1* mutant, which is from the Columbia ecotype, with the Lansberg *erecta* wild ecotype. The genetic linkage between the *hmc1* phenotype and various simple sequence length polymorphism (SSLP) and cleaved amplified polymorphic sequence (CAPS) markers listed in Online Resource 3 was subsequently analyzed with the F2 generation of the crossed lines. Finally, we mapped the *hmc1* mutation to a 1.8 Mb region on chromosome 4, a region that covers the centromere of this chromosome and contains approximately 130 open reading frames. We chose 25 open reading frames encoding putative chloroplast-targeted proteins whose expression was detected by microarray experiments according to the microarray data deposited in the public database (TAIR: http://www.arabidopsis.org/). All sequences were individually analyzed and we finally identified a mutation in the *AtNAP1* (At4g04770) locus encoding the SufB protein (Xu et al. 2005). The point mutation created a single base pair change from C to T at nucleotide position 778 within this gene, resulting in an amino acid substitution from a

conserved proline (P238) to leucine.

Complementation of *hmc1* with the cDNA clone for SufB

To verify that the mutation in the *AtNAP1* locus caused the *hmc1* phenotype, we introduced a cDNA clone for SufB under the control of a constitutive cauliflower mosaic virus 35S promoter into the *hmc1* mutant. In the resulting 35S-*AtNAP1*/*hmc1* lines, HMChl accumulation was suppressed to the wild type level (Fig. 7, Table 1). The reduction in plant size and low pigmentation were also rescued in these lines. Therefore, we concluded that the mutation in the *AtNAP1* locus conferred the *hmc1* phenotype to the plants.

Effect of the mutation of AtNAP1 on protein levels of ferredoxin and PaO

SUF (mobilization of sulfur) is one of the Fe-S cluster assembly systems in bacteria (Fontecave et al. 2005). SufB, SufC and SufD form a complex which participates in constructing and transferring the Fe-S cluster (Layer et al. 2007). Chloroplasts employ the same system composed of AtNAP1, AtNAP6 and AtNAP7, which are the counterparts of SufB, SufC and SufD, respectively, in *Arabidopsis* (Xu and Moller 2008). Proteins homologous to SufS, SufB, SufE and SufA are also found in the *Arabidopsis* genome (Xu and Moller 2006). Mutation in the *AtNAP1* locus might result in impairment of iron-sulfur formation. It has been reported that HAR and PaO use reduced ferredoxin for the reactions, and PaO contains an iron-sulfur center (Hörtensteiner 2006, 2009). A possible explanation for the accumulation of HMChl and pheophorbide *a* in the *hmc1* mutant is that ferredoxin and PaO are not sufficiently formed in *hmc1* due to mutation in the *AtNAP1* gene. We therefore determined ferredoxin and PaO by western blotting. However, there was no significant reduction in the protein levels of ferredoxin and PaO between the wild type and *hmc1* mutant (Fig. 8). The

PaO protein level was rather increased in the *hmc1* mutant. We speculate that the *hmc1* mutation didn't directly impair the synthesis of PaO, but enhanced PaO accumulation through an unidentified mechanism in a feedback manner.

Discussion

In this study, we first succeeded in isolating a mutant accumulating HMChl, an intermediate molecule of the chlorophyll cycle. In this mutant, HMChl accumulated at the level of 1-2% of total chlorophyll. It has been reported that the AtNAP1-deficient *laf6* mutant had an proximately twofold increase in protoporphyrin IX, a precursor of heme and chlorophyll, compared to that in the wild type (Moller et al. 2001). However, in our experiments, we could not find an increase in the protoporphyrin IX level. This might be due to the differences in growth conditions or the expression level of the *AtNAP1* gene between *laf6* and *hmc1*. We could not find other intermediate molecules of chlorophyll synthesis in *hmc1*. Mutants that have defects in chlorophyll metabolism have been reported to accumulate intermediate tetrapyrrole molecules such as uroporphyrinogen III (Hu et al. 1998), coproporphyrinogen III (Mock et al. 1999), protoporphyrinogen IX (Papenbrock et al. 2001) and pheophorbide *a* (Tanaka et al. 2003). These mutants exhibited necrotic phenotypes. This is because these tetrapyrrole pigments generate $^1O_2$ under light conditions. However, the phenotype of *hmc1* was different from these mutants and necrosis was not observed in *hmc1*, although an intermediate molecule, HMChl, accumulated in a large amount. It is possible that HMChl was incorporated into chlorophyll protein complexes and functions as a light-harvesting pigment, because the molecular structure and absorbance spectra of HMChl are similar to those of chlorophyll *a* and chlorophyll *b*, suggesting similar photosynthetic functions of HMChl as other chlorophylls. In this case, when HMChl absorbs light energy, excited energy is transferred

to neighboring pigments and does not produce reactive oxygen species. This assumption is also supported by results of our preliminary experiments showing that HMChl was incorporated into various chlorophyll-protein complexes in *hmc1* (data not shown). We speculate that the growth retardation and pale green phenotypes of *hmc1* may be a result of inefficient Fe-S cluster synthesis in this mutant. Our speculation is based on the observations with *atnap7* and the *hmc1/nol/nyc1* triple mutant in which both mutants do not accumulate HMChl but they still show growth retardation and pale green leaves. Another interesting phenotype of the *hmc1* mutant is the accumulation of pheophorbide *a*, a degradation intermediate of chlorophyll, when the mutant is incubated in the dark. In contrast to the accumulation of HMChl, accumulation of pheophorbide *a* was accompanied by a severe cell death phenotype, which is consistent with the result of a previous study showing that pheophorbide *a* induces light-independent cell death (Hirashima et al. 2009).

HMChl is an intermediate molecule of chlorophyll *b* synthesis. CAO carries out two successive oxygenation reactions and converts chlorophyll *a* to chlorophyll *b*, and the first oxygenation reaction produces HMChl (Oster et al. 2000). Result of in vitro experiments showed that when chlorophyllide *a* was incubated with recombinant CAO expressed in *E. coli*, 7-hydroxymethyl chlorophyllide *a* was accumulated in addition to chlorophyllide *b* in the reaction mixture (Oster et al. 2000). From these experiments, the possibility that HMChl was released from CAO and accumulated in *hmc1* cannot be excluded. The same situation is true for chlorophyll *b* to chlorophyll *a* conversion because HMChl and chlorophyll *a* accumulated when chlorophyll *b* was incubated with plastids (Ito et al. 1996). Therefore, HMChl in the *hmc1* mutant derives chlorophyll *a* to chlorophyll *b* conversion and/or chlorophyll *b* to chlorophyll *a* conversion. The genetic experiments clearly showed that mutation of chlorophyll *b* reductase, which produces HMChl from chlorophyll *b*, rescued the HMChl accumulating phenotype of *hmc1*, indicating that HMChl was produced during chlorophyll *b* to chlorophyll *a* conversion. From these experiments, we concluded that the reduction of

HMChl in the chlorophyll cycle is affected in *hmc1*. However, it should be noted that HAR is not completely inactivated in *hmc1*, as it was evident from the observations that chlorophyll *b* still decreased during senescence (see online resource 2). This phenotype is in contrast to the mutant of chlorophyll *b* reductase in which chlorophyll *b* does not decrease during senescence.

The *hmc1* mutant has a mutation in the *AtNAP1* gene, which has high sequence similarity to SufB (Xu et al. 2005). We are assuming that *hmc1* is neither loss-of-function nor gain-of-function. We observed that a loss-of-function allele of the *AtNAP1* locus is embryonic lethal (data not shown) unlike *hmc1*. If the *hmc1* mutation causes a gain of function, we would have expected it was dominant, but it was indeed recessive. It has been reported that SufB is involved in the assembly of iron-sulfur clusters in bacteria. There are three bacterial systems of iron-sulfur cluster formation (Bandyopadhyay et al. 2008), NIF (nitrogen fixation), ISC (iron sulfur cluster) and SUF (mobilization of sulfur). *Arabidopsis* chloroplasts have a complete SUF system. In bacteria, the SUF system consists of SufA, SufB, SufC, SufD, SufS and SufE (Fontecave et al. 2005). SufB, SufD and SufC are evolutionary conserved and form a complex. According to a recent hypothesis, the SufC/S complex donates sulfur to the SufB/SufD/SufC complex and SufB acts as a site for iron-sulfur cluster assembly (Layer et al. 2007). In *Arabidopsis* chloroplasts, AtNAP1, AtNAP6 and AtNAP7, which correspond to SufB, SufD and SufC in the bacterial system, also form a complex (Xu et al. 2005). Considering these results, it is reasonable to assume that the AtNAP1-AtNAP6-AtNAP7 complex is involved in iron-sulfur cluster formation in *Arabidopsis*. Although HAR has not been identified and our knowledge of its enzymatic character is very limited, it was shown by an in vitro experiment with the chloroplast that HAR accepts electrons from ferredoxin (Scheumann et al. 1998). Interestingly, PaO contains a 2S-2Fe cluster and uses ferredoxin as a reducing power. If the synthesis of ferredoxin and PaO is impaired due to the low activity of iron-sulfur formation, HMChl and pheophorbide

a would not be efficiently converted to chlorophyll *a* and red chlorophyll catabolite, respectively, resulting in the accumulation of HMChl and pheophorbide *a*. However, a western blotting experiment clearly showed that the levels of ferredoxin and PaO were not lowered in the *hmc1* mutant. Therefore, accumulation of HMChl and pheophorbide *a* is not simply due to the low activity for formation of an iron-sulfur cluster of PaO and ferredoxin. Thus, two hypotheses can be proposed for the accumulation of HMChl and pheophorbide *a*. The first hypothesis is that the *hmc1* mutation specifically affects the synthesis of the iron-sulfur protein which is involved in the regulation of both HAR and pheophorbide *a* oxygenase. The other hypothesis is that AtNAP1 regulates HAR and PaO activity by other mechanisms besides Fe-S cluster formation. AtNAP1 is slightly different from corresponding proteins of bacterial SufB, since it does not only interact with AtNAP7 but can form a homodimer and shows iron-stimulated ATPase activity (Xu et al. 2005). The Bio-Array Resource database (http://bbc.botany.utoronto.ca/) shows that *AtNAP1* mRNA level is high in senescent leaves compared to that in green leaves. According to the result of our western blotting analysis, accumulation of AtNAP1 protein was greatly enhanced when the senescence was induced by dark incubation (Online Resource 4). This expression profile of *AtNAP1* appears contrary to expectations that Fe-S clusters should be more actively synthesized during chloroplast formation than in the senescent phase. Actually, mRNA levels of other members of the NAP complexes are high in green leaves (Online Resource 4). From these results, it is reasonable to assume that AtNAP1 has an additional function besides cluster formation by the AtNAP1-AtNAP6-AtNAP-7 complex.

It should be noted that two different intermediate molecules of the chlorophyll degradation pathway accumulated by a single mutation, suggesting that chlorophyll degradation is regulated by a common mechanism and/or chlorophyll degradation enzymes interact with each other. Chlorophyll degradation enzymes might be coordinately regulated by an unknown mechanism. Analysis of the *hmc1* mutant should provide a clue for understanding the concerted regulation of

chlorophyll degradation and AtNAP1 function.

Acknowledgements

We thank Dr. Nozomi Nagata for HPLC analysis and we thank Junko Kishimoto and Masumi Hirashima for their excellent technical assistance in electron microscopy and other experimental procedures. We are grateful to Dr. Atsushi Takabayashi for critical reading of the manuscript. We thank the Arabidopsis Information Resource (TAIR), Arabidopsis Biological Resources (ABRC) and GABI-KAT for providing bioinformatics resources and the mutant seeds (SALK_111333, SALK_091664 and AL759262). This work was supported by a Grant-in-Aid for Creative Scientific Research (No. 17GS0314 to A. T.) and Grant-in-Aid for Scientific Research (No. 68700307 to R. T.) from the Ministry of Education, Culture, Sports, Science, and Technology of Japan.

References

Bandyopadhyay S, Chandramouli K, Johnson MK (2008) Iron-sulfur cluster biosynthesis. Biochem Soc Trans 36: 1112-1119

Fontecave M, Choudens SO, Py B, Barras F (2005) Mechanisms of iron-sulfur cluster assembly: the SUF machinery. J Biol Inorg Chem 10: 713-721

Fromme P, Melkozernov A, Jordan P, Krauss N (2003) Structure and function of photosystem I: interaction with its soluble electron carriers and external antenna systems. FEBS Lett 555: 40-44

Green BR, Durnford DG (1996) The chlorophyll-carotenoid proteins of oxygenic photosynthesis. Annu Rev Plant Physiol Plant Mol Biol 47: 685-714

Harper AL, von Gesjen SE, Linford AS, Peterson MP, Faircloth RS, Thissen MM, Brusslan JA (2004) Chlorophyllide *a* oxygenase mRNA and protein levels correlate with the chlorophyll *a/b* ratio in *Arabidopsis thaliana*. Photosynth Res 79: 149-159

Hellens RP, Edwards EA, Leyland NR, Bean S, Mullineaux PM (2000) pGreen: a versatile and flexible binary Ti vector for Agrobacterium-mediated plant transformation. Plant Mol Biol 42: 819-832

Horie Y, Ito H, Kusaba M, Tanaka R, Tanaka A (2009) Participation of chlorophyll *b* reductase in the initial step of the degradation of light-harvesting chlorophyll *a/b*-protein complexes in *Arabidopsis*. J Biol Chem 284: 17449-17456

Hörtensteiner S (2006) Chlorophyll degradation during senescence. Annu Rev Plant Biol 57: 55-77

Hu G, Yalpani N, Briggs SP, Johal GS (1998) A porphyrin pathway impairment is responsible for the phenotype of a dominant disease lesion mimic mutant of maize. Plant Cell 10: 1095-1105

Ito H, Ohtsuka T, Tanaka A (1996) Conversion of chlorophyll *b* to chlorophyll *a* via 7-hydroxymethyl chlorophyll. J Biol Chem 271: 1475-1479

Ito H, Takaichi S, Tsuji H, Tanaka A (1994) Properties of synthesis of chlorophyll *a* from chlorophyll *b* in cucumber etioplasts. J Biol Chem 269: 22034-22038

Ito H, Tanaka Y, Tsuji H, Tanaka A (1993) Conversion of chlorophyll *b* to chlorophyll *a* by isolated cucumber etioplasts. Arch Biochem Biophys 306: 148-151

Kobayashi Y, Kanesaki Y, Tanaka A, Kuroiwa H, Kuroiwa T, Tanaka K (2009) Tetrapyrrole signal as a cell-cycle coordinator from organelle to nuclear DNA replication in plant cells. Proc Natl Acad Sci U S A 106: 803-807

Kusaba M, Ito H, Morita R, Iida S, Sato Y, Fujimoto M, Kawasaki S, Tanaka R, Hirochika H, Nishimura M, Tanaka A (2007) Rice *NON-YELLOW COLORING1* is involved in light-harvesting complex II and grana degradation during leaf senescence. Plant Cell 19: 1362-1375

Layer G, Gaddam SA, Ayala-Castro CN, Ollagnier-de Choudens S, Lascoux D, Fontecave M, Outten FW (2007) SufE transfers sulfur from SufS to SufB for iron-sulfur cluster assembly. J Biol Chem 282: 13342-13350

Masuda T, Polle JE, Melis A (2002) Biosynthesis and distribution of chlorophyll among the photosystems during recovery of the green alga *Dunaliella salina* from irradiance stress. Plant Physiol 128: 603-614

Masuda T, Tanaka A, Melis A (2003) Chlorophyll antenna size adjustments by irradiance in *Dunaliella salina* involve coordinate regulation of chlorophyll *a* oxygenase (CAO) and *Lhcb* gene expression. Plant Mol Biol 51: 757-771

Matsumoto F, Obayashi T, Sasaki-Sekimoto Y, Ohta H, Takamiya K, Masuda T (2004) Gene expression profiling of the tetrapyrrole metabolic pathway in Arabidopsis with a mini-array system. Plant Physiol 135: 2379-2391

Mock HP, Heller W, Molina A, Neubohn B, Sandermann H, Jr., Grimm B (1999) Expression of uroporphyrinogen decarboxylase or coproporphyrinogen oxidase antisense RNA in tobacco induces pathogen defense responses conferring increased resistance to tobacco mosaic virus. J. Biol. Chem. 274: 4231-4238

Moller SG, Kunkel T, Chua NH (2001) A plastidic ABC protein involved in intercompartmental communication of light signaling. Genes Dev 15: 90-103

op den Camp RG, Przybyla D, Ochsenbein C, Laloi C, Kim C, Danon A, Wagner D, Hideg E, Gobel C, Feussner I, Nater M, Apel K (2003) Rapid induction of distinct stress responses after the release of singlet oxygen in Arabidopsis. Plant Cell 15: 2320-2332.

Oster U, Tanaka R, Tanaka A, Rüdiger W (2000) Cloning and functional expression of the gene encoding the key enzyme for chlorophyll b biosynthesis (CAO) from Arabidopsis thaliana. Plant J 21: 305-310

Papenbrock J, Mishra S, Mock HP, Kruse E, Schmidt EK, Petersmann A, Braun HP, Grimm B (2001) Impaired expression of the plastidic ferrochelatase by antisense RNA synthesis leads to a necrotic phenotype of transformed tobacco plants. Plant J 28: 41-50

Pattanayak GK, Biswal AK, Reddy VS, Tripathy BC (2005) Light-dependent regulation of chlorophyll b biosynthesis in chlorophyllide a oxygenase overexpressing tobacco plants. Biochem Biophys Res

Commun 326: 466-471

Rüdiger W (2002) Biosynthesis of chlorophyll b and the chlorophyll cycle. Photosynth Res 74: 187-193

Scheumann V, Schoch S, Rüdiger W (1998) Chlorophyll *a* formation in the chlorophyll *b* reductase reaction requires reduced ferredoxin. J Biol Chem 273: 35102-35108

Shimada Y, Tanaka A, Tanaka Y, Takabe T, Takabe T, Tsuji H (1990) Formation of chlorophyll-protein complexes during greening 1. Distribution of newly synthesized chlorophyll among apoproteins. Plant Cell Physiol 31: 639-647

Tanaka A, Ito H, Tanaka R, Tanaka NK, Yoshida K, Okada K (1998) Chlorophyll *a* oxygenase (CAO) is involved in chlorophyll *b* formation from chlorophyll *a*. Proc Natl Acad Sci U S A 95: 12719-12723

Tanaka R, Hirashima M, Satoh S, Tanaka A (2003) The *Arabidopsis-accelerated cell death* gene *ACD1* is involved in oxygenation of pheophorbide *a*: Inhibition of the pheophorbide *a* oxygenase activity does not lead to the "stay-green" phenotype in *Arabidopsis*. Plant Cell Physiol 44: 1266-1274

Tanaka R, Tanaka A (2005) Effects of chlorophyllide *a* oxygenase overexpression on light acclimation in *Arabidopsis thaliana*. Photosynth Res 85: 327-340

Tanaka R, Tanaka A (2007) Tetrapyrrole biosynthesis in higher plants. Annu Rev Plant Biol 58: 321-346

Vasilikiotis C, Melis A (1994) Photosystem II reaction center damage and repair cycle: chloroplast acclimation strategy to irradiance stress. Proc Natl Acad Sci U S A 91: 7222-7226

Vothknecht UC, Kannangara CG, Von Wettstein D (1998) Barley glutamyl $tRNA^{Glu}$ reductase: Mutations affecting haem inhibition and enzyme activity. Phytochem 47: 513-519

Xu XM, Adams S, Chua NH, Moller SG (2005) AtNAP1 represents an atypical SufB protein in Arabidopsis plastids. J Biol Chem 280: 6648-6654

Xu XM, Moller SG (2006) AtSufE is an essential activator of plastidic and mitochondrial desulfurases in Arabidopsis. EMBO J 25: 900-909

Xu XM, Moller SG (2008) Iron-sulfur cluster biogenesis systems and their crosstalk. Chembiochem 9: 2355-2362

Yamasato A, Nagata N, Tanaka R, Tanaka A (2005) The N-terminal domain of chlorophyllide *a* oxygenase confers protein instability in response to chlorophyll *b* accumulation in *Arabidopsis*. Plant

Cell 17: 1585-1597

Yang DH, Andersson B, Aro EM, Ohad I (2001) The redox state of the plastoquinone pool controls the level of the light-harvesting chlorophyll a/b binding protein complex II (LHC II) during photoacclimation. Photosynth Res 68: 163-174

Zapata M, Rodriguez F, Garrido JL (2000) Separation of chlorophylls and carotenoids from marine phytoplankton: a new HPLC method using a reversed phase C-8 column and pyridine-containing mobile phases. Marine Ecology-Progress Series 195: 29-45 Yang et al. 2001

Table

	Chlorophyll *a* (nmol/gFW)	Chlorophyll *b* (nmol/gFW)	HMchl (nmol/gFW)	Total chlorophyll (nmol/gFW)	Chlorophyll *a/b* ratio
Wild type	1673±300	525±98	0.16±0.34	2198±398	3.2±0.02
hmc1	1060±121	346±38	26.6±2.9	1406±159	3.1±0.09
35S-*AtNAP1/hmc1*	1543±35	506±12	0.17±0.18	2049±47	3.0±0.03

Table 1 Chlorophyll contents in mutants. Leaves from the third whorl were harvested from 3-week-old plants and their chlorophyll contents were measured by HPLC as described in Materials and Methods. Error bars indicate the SD of five independent samples from a single harvest.

Figure legends

Fig. 1 An overview of the chlorophyll cycle. Higher plants utilize two chlorophyll species, chlorophyll *a* and chlorophyll *b*, for photosynthesis. These chlorophyll species are converted to one another in order to balance the ratios between chlorophyll *a* and *b*. Chlorophyll *a* is first synthesized from glutamate by 15 enzymatic steps, which are depicted in the figure. In the next step, chlorophyllide *a* oxygenase (CAO) converts chlorophyll *a* to chlorophyll *b* via HMChl. Chlorophyll *b* can be converted to HMChl again by chlorophyll *b* reductase, an enzyme which is encoded by the *NYC1* and *NOL* genes in *Arabidopsis* (Kusaba et al. 2007). HMChl is returned to chlorophyll *a* by HAR, an enzyme which was shown to be ferredoxin-dependent (Scheumann et al. 1998). Upon leaf senescence, chlorophyll *b* is converted to chlorophyll *a*, which is then degraded by pheophytin-pheophorbide hydrolase, pheophorbide *a* oxygenase and red chlorophyll catabolite reductase (Hörtensteiner 2009) to form red chlorophyll catabolite. This compound is further metabolized to non-fluorescent chlorophyll catabolites (not illustrated).

Fig. 2 **a-b** Visible phenotype and HPLC chromatograms of WT and *hmc1*. **a** HPLC chromatograms showing the accumulation of various chlorophyll derivatives. Peak 1, HMChl. Peak 2, chlorophyll *b*. Peak 3, chlorophyll *a*. Peak 4, pheophytin *a*. The scales of chromatograms were normalized with the heights of the chlorophyll *b* peaks. **b** Comparison of the plants analyzed in this study. Plants were grown for 35 days and their leaf colors and sizes were compared.

Fig. 3 **a-c** Chlorophyll accumulation in the *hmc1* mutant during the vegetative phase. The error bars indicate the standard deviation for five samples from a single harvest. The third leaf whorl was harvested at the time indicated and immediately frozen in liquid nitrogen for pigment analysis as described in Materials and Methods. **a** HMChl contents in WT (white circles) and *hmc1* (filled squares) on a leaf fresh weight basis. **b** Total chlorophyll level (chlorophyll *a* + chlorophyll *b* + HMChl) in WT (white circles) and *hmc1* (filled squares) on a leaf fresh weight basis. **c** Chlorophyll *a* to *b* ratios in WT (white circles) and *hmc1* (filled squares). Error bars represent the standard deviation of 5 samples from a single harvest.

Fig. 4 HPLC chromatograms for wild type, *hmc1* and *hmc1/nyc1/nol*. Peak 1, HMChl. Peak 2, chlorophyll *b*. Peak 3, chlorophyll *a*. Peak 4, pheophytin *a*. The scales of chromatograms were normalized with the heights of the chlorophyll *b* peaks.

Fig. 5 Pigment accumulation in wild type and *hmc1* during leaf senescence. Peak 1, Pheophorbide *a*. Peak 2, HMChl. Peak 3, chlorophyll *b*. Peak 4, chlorophyll *a*. Peak 5, pheophytin *a*. The scales of chromatograms were normalized with the heights of the chlorophyll *b* peaks.

Fig. 6 **a-f** Electron microscopic observation of WT and *hmc1* chloroplasts. Ultrastructure of WT (**a**) and *hmc1* (**b**) cells before dark incubation. Ultrastructure of WT (**c**) and *hmc1* (**d**,**e** and **f**) cells after dark incubation. **d** The cell structure was completely destroyed. **e** The envelope membranes of the chloroplast appeared to have collapsed, but thylakoid membranes remained intact. **f** An apparently healthy cell was adjacent to the collapsed cells in *hmc1*. Scale bar = 500 nm.

Fig. 7 HPLC chromatograms for wild type, *hmc1* and 35S-*AtNAP1*/*hmc1* lines. Peak 1, HMChl. Peak 2, chlorophyll *b*. Peak 3, chlorophyll *a*. Peak 4, pheophytin *a*. The scales of chromatograms were normalized with the heights of the chlorophyll *b* peaks.

Fig. 8 **a-b** Immunoblot analysis of ferredoxin and PaO levels in WT and *hmc1*. Leaf ferredoxin (**a**) and PaO (**b**) were detected with an anti-ferredoxin or anti-PaO antibody as described in Materials and Methods. A protein extract equivalent to 0.2 mg fresh leaf weight was loaded per lane (**a-b**).

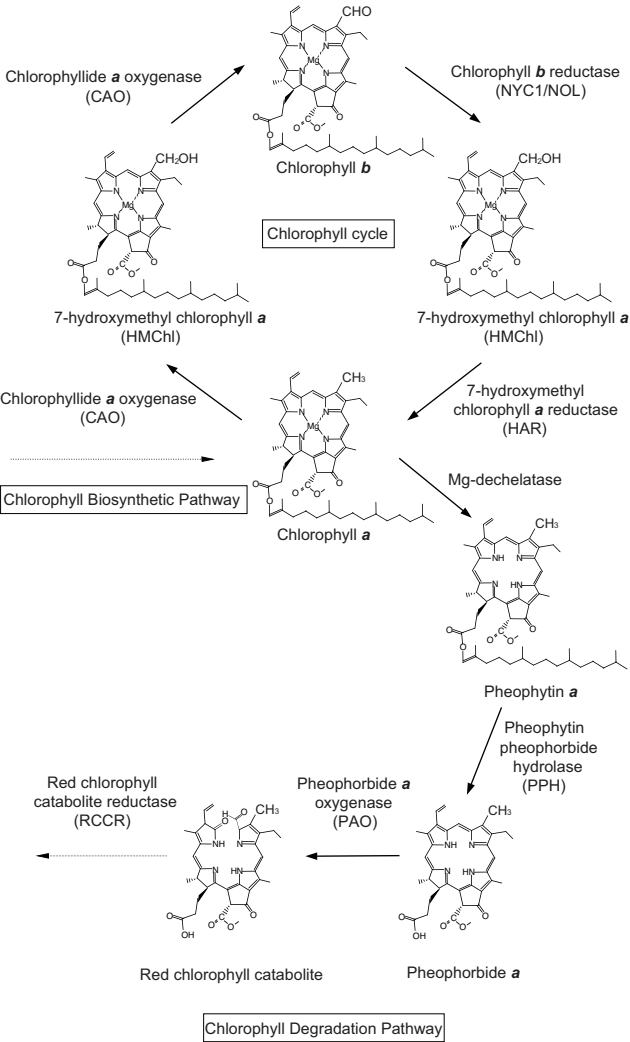
Chlorophyllide a oxygenase (CAO)
Chlorophyll b reductase (NYC1/NOL)
Chlorophyll b
Chlorophyll cycle
7-hydroxymethyl chlorophyll a (HMChl)
7-hydroxymethyl chlorophyll a (HMChl)
Chlorophyllide a oxygenase (CAO)
7-hydroxymethyl chlorophyll a reductase (HAR)
Chlorophyll Biosynthetic Pathway
Mg-dechelatase
Chlorophyll a
Pheophytin a
Pheophytin pheophorbide hydrolase (PPH)
Red chlorophyll catabolite reductase (RCCR)
Pheophorbide a oxygenase (PAO)
Red chlorophyll catabolite
Pheophorbide a
Chlorophyll Degradation Pathway

a

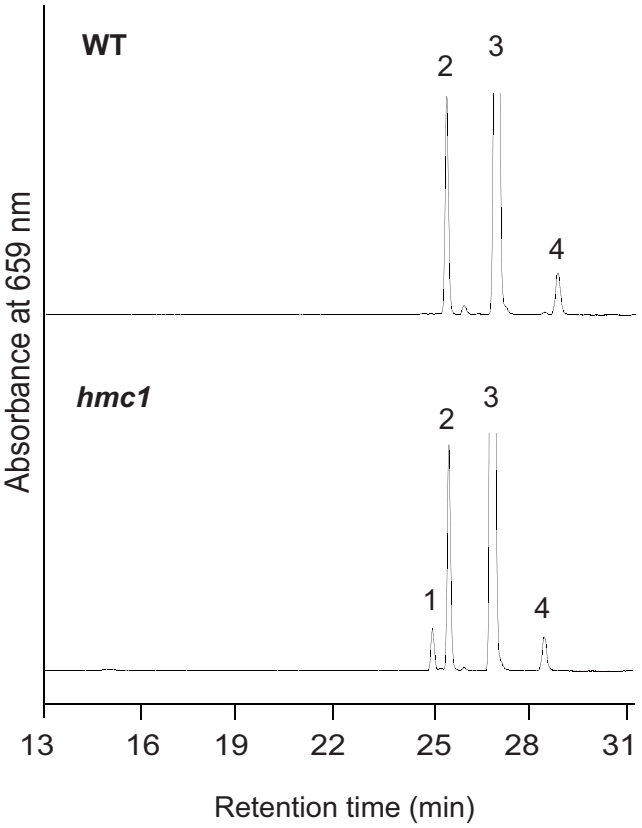
WT
2
3
4
hmc1
2
3
1
4
Absorbance at 659 nm
13
16
19
22
25
28
31
Retention time (min)

b

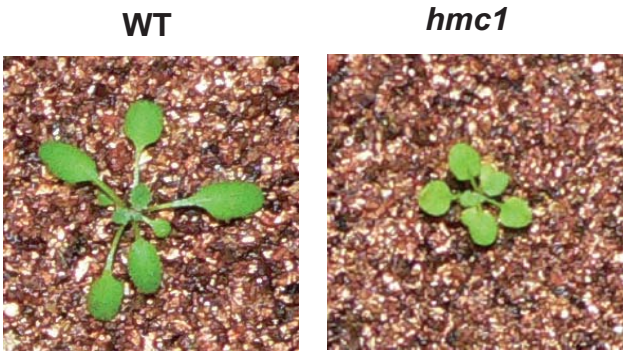
WT
hmc1

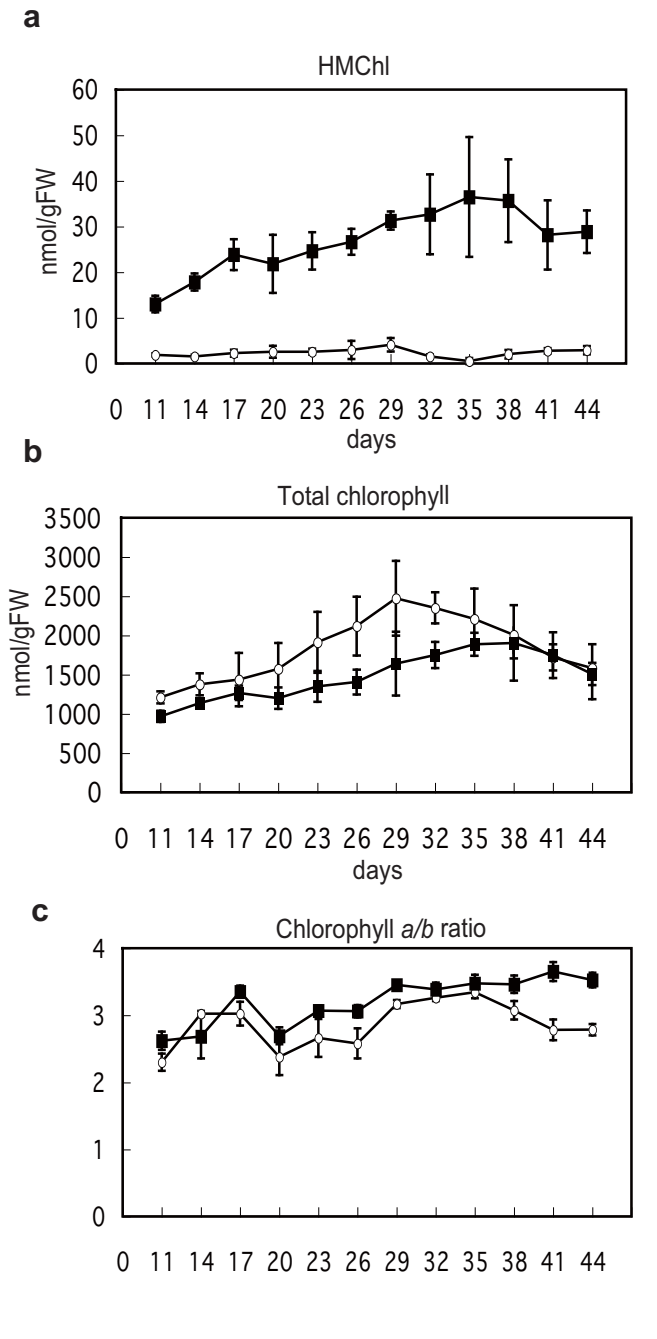
a
HMChl
nmol/gFW
60
50
40
30
20
10
0
0 11 14 17 20 23 26 29 32 35 38 41 44
days
b
Total chlorophyll
nmol/gFW
3500
3000
2500
2000
1500
1000
500
0
0 11 14 17 20 23 26 29 32 35 38 41 44
days
c
Chlorophyll a/b ratio
4
3
2
1
0
0 11 14 17 20 23 26 29 32 35 38 41 44

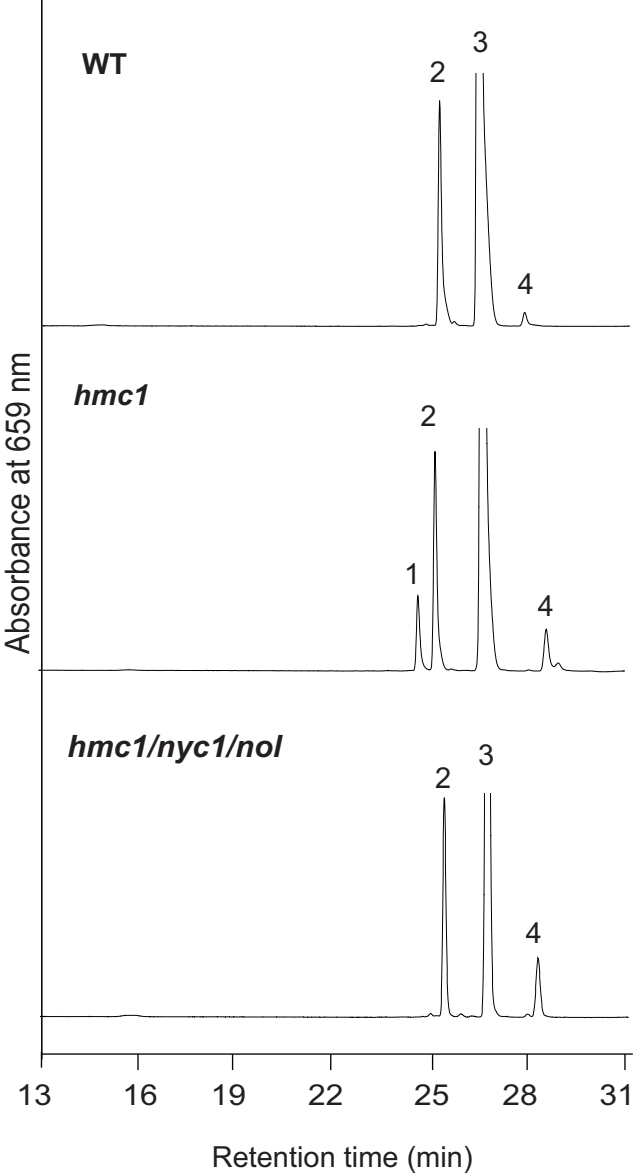
WT
2
3
4
hmc1
1
2
4
hmc1/nyc1/nol
2
3
4
Absorbance at 659 nm
13
16
19
22
25
28
31
Retention time (min)

Fig.5

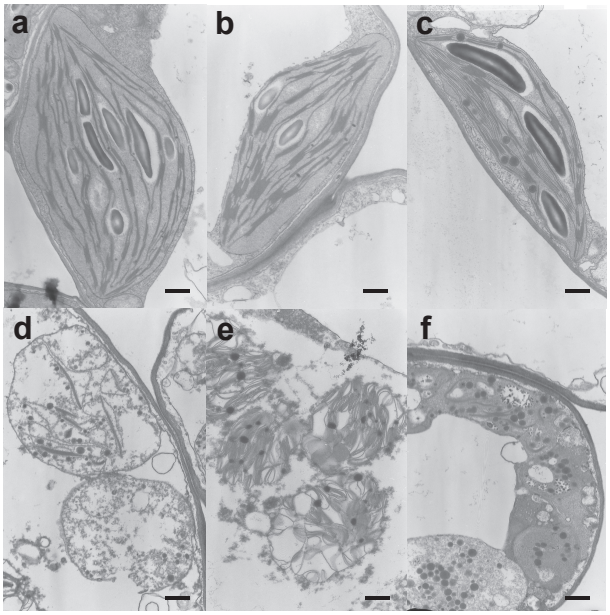

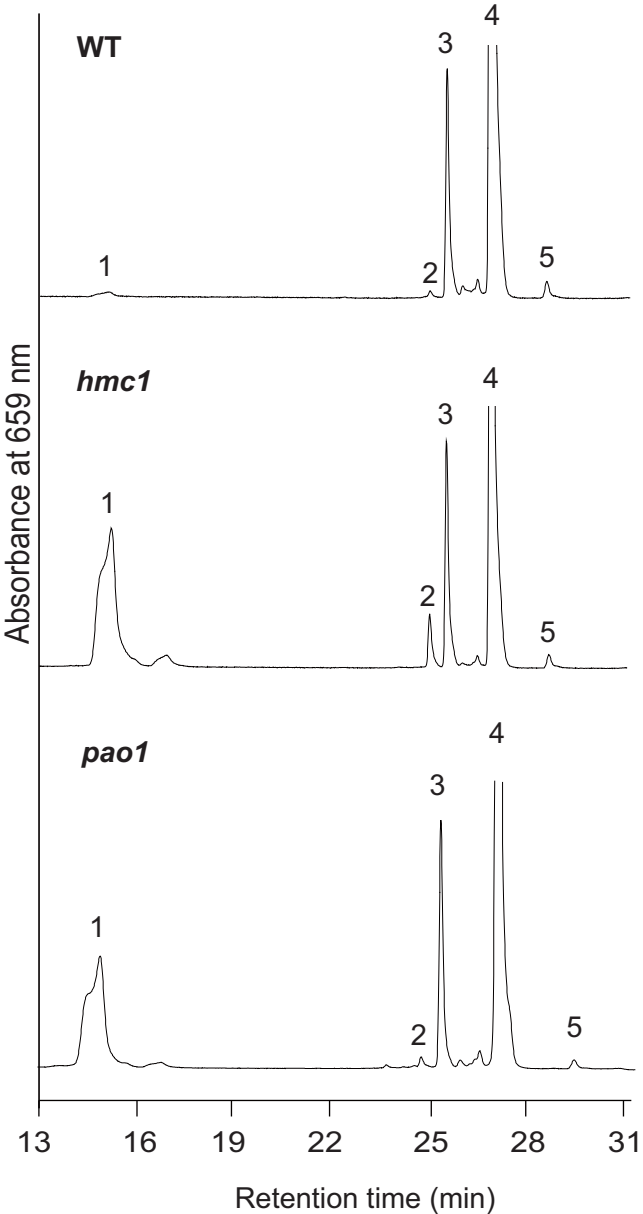
WT
1
2
3
4
5
hmc1
1
2
3
4
5
pao1
1
2
3
4
5
Absorbance at 659 nm
13
16
19
22
25
28
31
Retention time (min)

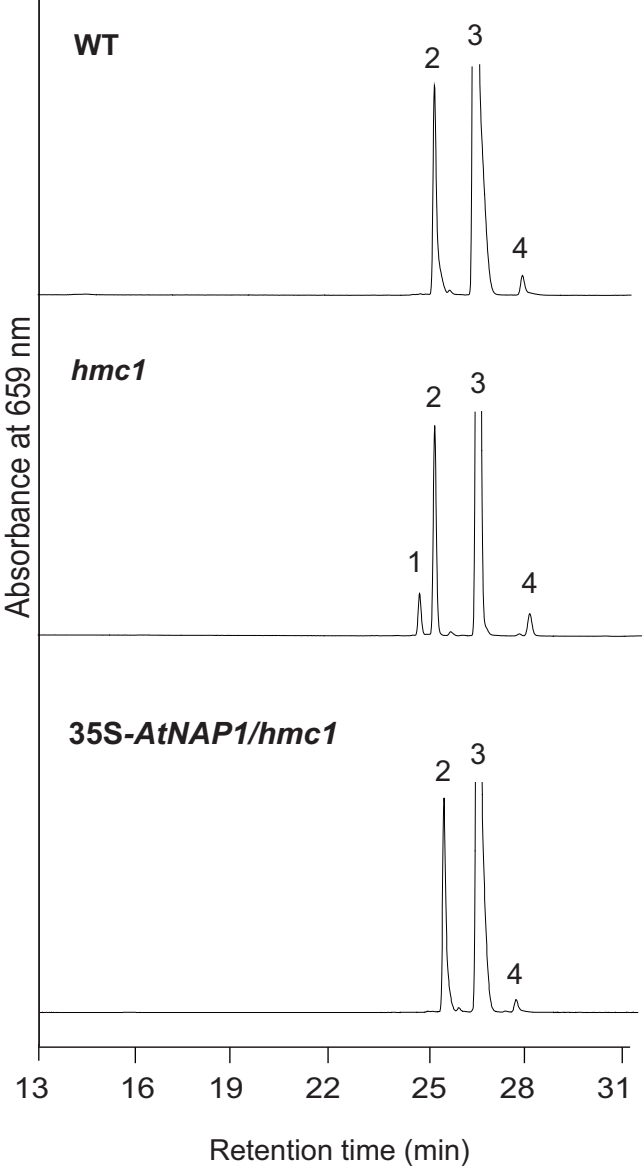
WT
2
3
4
hmc1
1
2
3
4
35S-AtNAP1/hmc1
2
3
4
Absorbance at 659 nm
13
16
19
22
25
28
31
Retention time (min)

a

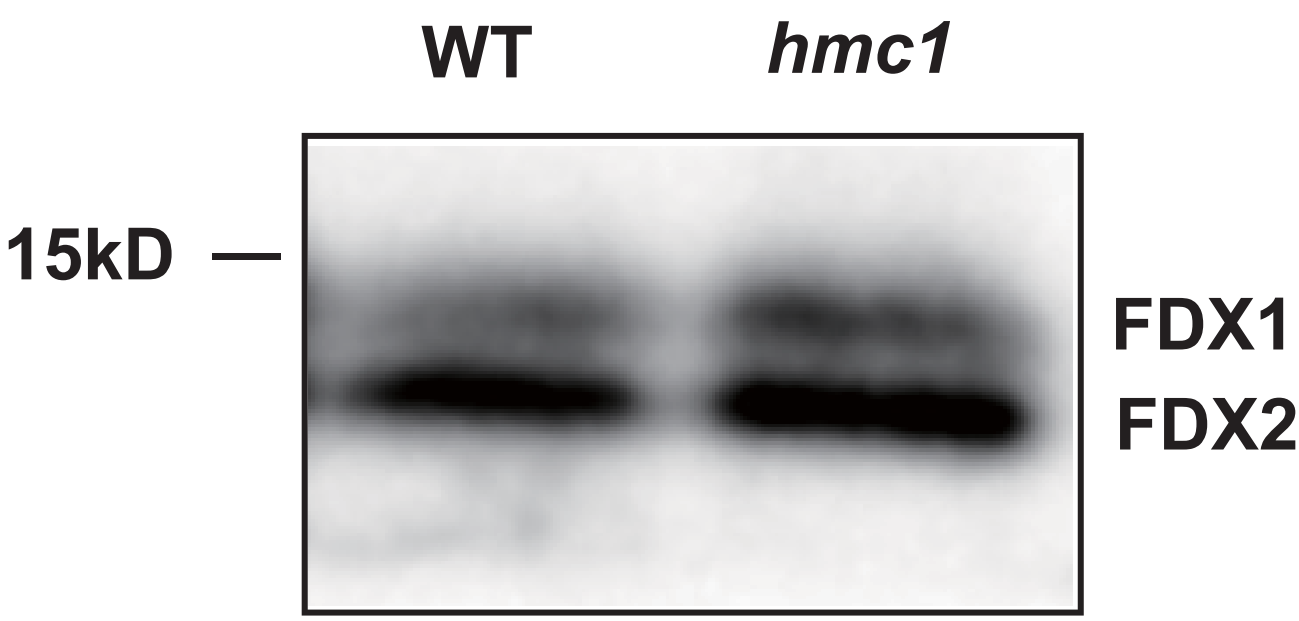
WT
hmc1
15kD
FDX1
FDX2

b

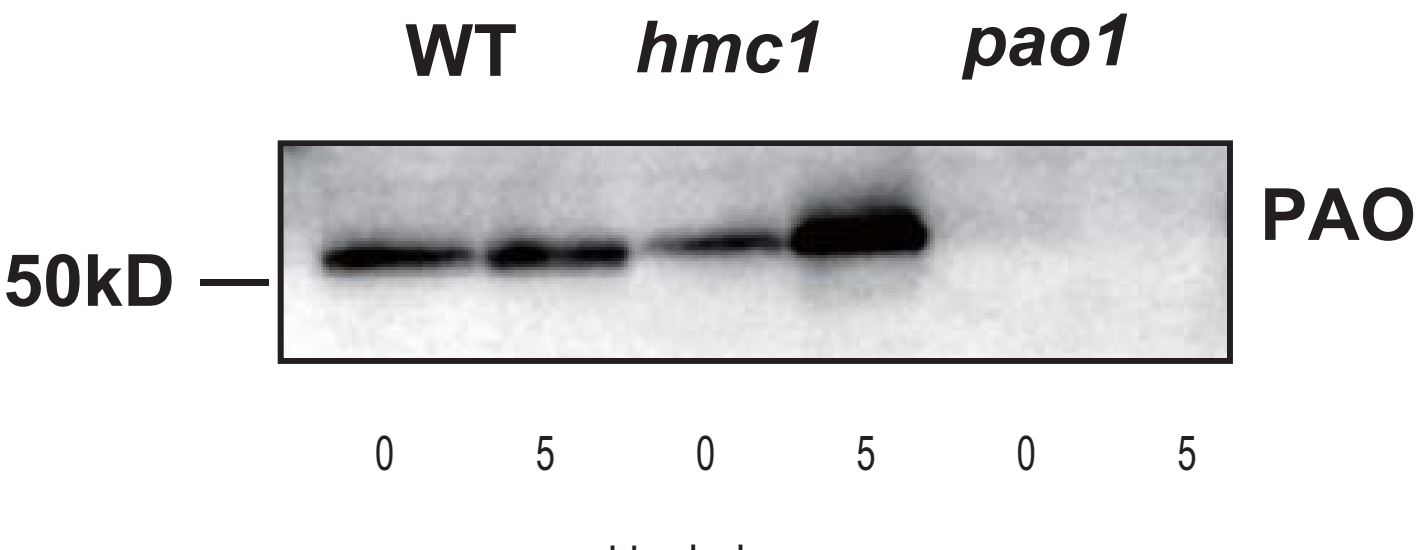
WT
hmc1
pao1
50kD
PAO
0
5
0
5
0
5
d in darkness